Journal of the Korean Physical Society, Vol. 56, No. 2, February 2010, pp. 548∼553

Light Efficiency of the Dependence of Fringe-field Switching Mode on the of the Dielectric Anisotropy of Liquid Crystal for Various Values of the Cell Gap and the Rubbing Angle

Jun Ho Jung, Kyung Su Ha, Mina Chae, Anoop Kumar Srivastava and Seung Hee Lee*
Polymer Fusion Research Center, Department of Polymer-Nano Science and Technology, Chonbuk National University, Chonju 561-756

Seung-Eun Lee
Merck Advanced Technologies Ltd. 1173-2, Pyongtaek 451-822

Hee Kyu Lee
Polymer Fusion Research Center, Department of Polymer-Nano Science and Technology, Chonbuk National University, Chonju 561-756, and Merck Advanced Technologies Ltd. 1173-2, Pyongtaek 451-822

(Received 1 September 2009, n final form 7 January 2010)

The light efficiency of the homogeneously aligned liquid crystal (LC) mode driven by fringe electric fields depends on the magnitude of the dielectric anisotropy when using a LC with positive dielectric anisotropy. However, this dependency is not observed when using a LC with negative dielectric anisotropy. This difference is mainly associated with the molecular reorientation especially in the tilt angle of the LC between the edges and the centers of the pixel electrodes in the voltage-on state. This paper explores the dependence of the light efficiency of the device on the magnitude of the dielectric anisotropy of the LC for both types of the LCs as functions of other cell parameters such as the rubbing angle and the cell gap.

PACS numbers: 42.30.Kr, 42.40.Ht, 42.30.Kq
Keywords: Fringe-field switching, Light efficiency, Dielectric anisotropy, Rubbing angle
DOI: 10.3938/jkps.56.548

I. INTRODUCTION

Nowdays, liquid crystal displays (LCDs) are major displays among all types of information displays. The image quality of LCDs has been greatly improved in recent years owing to the development of new LCD modes, such as multi-domain vertical alignment (MVA) [1,2], in-plane switching (IPS) [3–5], and fringe-field switching (FFS) [6–10]. In general, light modulation of the LCDs occurs either by phase retardation or a polarization rotation effect using the LC layers. The light efficiency of a LC cell mainly depends on the retardation of the LC layer. In the MVA mode, only a LC with negative dielectric anisotropy (-LC) is used while the IPS mode mainly uses a LC with a positive dielectric anisotropy (+LC). For both devices, the light efficiency does not depend on the magnitude of the dielectric anisotropy at all.

The FFS mode is known to exhibit a wide viewing angle and a high transmittance as compared to other devices. Until now, many reports on the switching principles of the device and on improve made in electro-optic characteristics of the FFS device have been made. The light efficiency of the device is known to depend on the rubbing direction [11], electrode structure [12,13], cell's retardation [14,15], cell gap [16,17], and the sign of the dielectric anisotropy [18]. Recently, magnitude of the dielectric anisotropy with +LC was reported to affects light efficiency of the device [19].

In the FFS device, the light efficiency is associated with other cell parameters, such as the rubbing angle and the cell gap; furthermore, its behavior can be totally different when using -LC. Therefore, this paper investigates how the light efficiency of the FFS mode is affected by the magnitude of a dielectric anisotropy of LC for various rubbing angles and cell gaps for both +LC and -LC.

II. SWITCHING PRINCIPLE OF THE FFS MODE AND SIMULATION CONDITIONS

*E-mail: lsh1@chonbuk.ac.kr

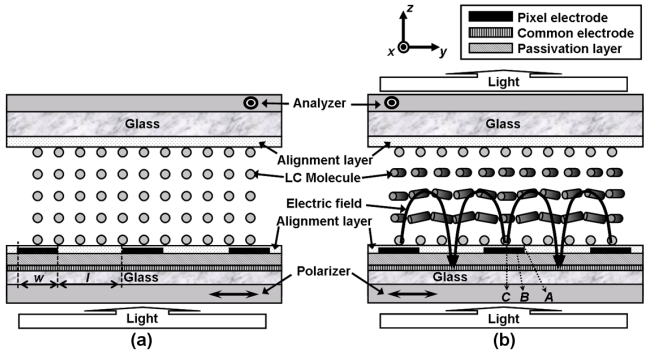

Fig. 1. Schematic cell structure with molecular orientation in the fringe-field switching mode; (a) off state and (b) on state.

In the IPS mode in which the optic axis of the LC coincides with one of the axes of the crossed polarizer; the normalized light transmission of the device can be determined by using the following equation;

$$T/T_0 = \sin^2 2\Psi(V) \sin^2(\pi d \Delta n_{eff}(V)/\lambda), \tag{1}$$

where Ψ is the voltage-dependent angle between the tr*ansmiss*ion axis of the crossed polarizer and the LC director, Δn_{eff} is a voltage-dependent effective birefringence, d is the cell gap, and λ is the wavelength of the incident light. Before applying a bias voltage, the Ψ is zero; thus, the cell appears black. With a bias voltage, the optic axis of the LC starts to deviate from the polarizer axis; hence, transmittance starts to occur.

Figure 1 shows a side-view schematic of the cell structure and orientation of the LC in the off and the on statesin the FFS cell, in which both the pixel and the common electrodes exist on the bottom substrate with a passivation layer between them. The pixel electrode is patterned in the form of the slit. Here, both the common and the pixel electrodes are made of transparent materials. In the device, the LCs are homogeneously aligned in an initial state with the optic axis of the LC coinciding with one of the axes of the crossed polarizes so that the cell appears dark in the off state, as in the IPS mode. When a voltage is applied between the pixel and the common electrodes, fringe electric fields, which have both horizontal (E_y) and vertical (E_z) field components are generated, as indicated in Fig. 1. This field rotates LC; thus, the LC director deviates from the polarizer's axis, giving rise to transmittance.

The vertical electric field (E_z) is well known to be much stronger at position B (between the center and the edge of the electrode) than at position A (electrode's edge) whereas the horizontal field intensity of E_y is much stronger at position A than at position B; both E_z and E_y are zero at the center of the electrode, *i.e.*, at position C. Consequently, the tilt angle is largest at position B than at the other two positions because of E_z whereas the dielectric torque to rotate the homogenously aligned LC is largest at electrode position A compared to the other two positions because of E_y; thus, the rotated (twist) angle of the LC director due to the field will be largest at position A. Further the electric field continues to decreasing from the bottom to the top of the LC layer. Thus, LC molecules are twisted from the bottom to the top of the LC layer continuously, as in the twisted nematic device [20,21]; thus, light modulation occurs because of polarization rotation. As the electric field is zero at the center of the electrode position C, the orientation of the LC molecules at position C is due to the elastic torque of its neighboring molecules. Furthermore, the LC molecules near the alignment layer do not rotate as much as they do at the middle of the LC layer because of the surface anchoring energy between the LC molecules and the alignment layer. In other words the LC molecules rotate more at the middle of the LC layer than at the bottom and the top substrates, similar to the IPS device [14]; hence, light modulation occurs because of phase retardation.

Due to different LC orientations in the on state, the light modulation can be different, depending upon the electrode position; thus, the transmittance in Eq. (1) can be modified as follows [16]:

$$T/T_0 = \boldsymbol{\alpha} \sin^2 2\Psi \sin^2(\boldsymbol{\beta}\pi d\Delta n/\lambda) + \gamma(1 - \frac{\sin^2(\pi/2\sqrt{1+(2\delta d\Delta n/\lambda)^2})}{1+(2\delta d\Delta n/\lambda)^2}) , \tag{2}$$

where α, β, γ, and δ are fitting parameters related to the transmittance and effective cell retardations. The first term in Eq. (2) comes from Eq. (1), and the second term is incorporated from Gooch and Terry's transmittance equation for the TN mode.

In order to calculate the potential and the distribution of the LC director as a function of the voltage, we performed a computer simulation by using the commercially available software "LCD Master" (Shintech, Japan). In the simulation, two different kinds of energy are considered, namely the elastic energy and the electric energy. In the FFS mode, deformation of the LC director is associated with the splay k_{11}, the twist k_{22}, and the bend k_{33} elastic constants; thus, the free energy $F_{elastic}$ per unit volume with respect to changes of elasticity is given by

$$F_{elastic} = \frac{1}{2}k_{11}(\mathbf{div}\boldsymbol{n}) + \frac{1}{2}k_{22}(\boldsymbol{n}\cdot rot\boldsymbol{n}) + \frac{1}{2}k_{33}|\boldsymbol{n}\times\mathbf{rot}\boldsymbol{n}|^2 \tag{3}$$

with $\mathbf{n}$ being the unit vector of the director,

$$|\mathbf{n}| = 1 \tag{4}$$

In the presence of an electric field, the electrical energy $F_{elastic}$ per unit volume due to the electric field is given by

$$F_{elastic} = \frac{1}{2}\varepsilon \boldsymbol{E} \cdot \boldsymbol{E}. \quad (5)$$

ϵ is the dielectric tensor of the LC, and E is the electric field. Then, the total free energy per unit volume F (Gibbs free energy) is given by

$$F = F_{elastic} - F_{electric}. \quad (6)$$

The LC director distribution is calculated by minimizing the Gibbs free energy.

To calculate the transmittance of the FFS cell as a function of the LC orientation, we applied a 2 × 2 extended Jones matrix [22], assuming the transmittances of the single and the parallel polarizers to be 41% and 35%, respectively. In the computer simulations, the width of the pixel electrode and the distance between them were 4 μm and 6 μm, respectively. The thickness of the insulation layer between the electrodes was 6300 Å, and the cell gap was 3.6 μm. Various types of LCs having positive dielectric anisotropy ($\Delta\epsilon$ = 2, 5, 9.4, 13 at 1 kHz) and negative dielectric anisotropy ($\Delta\epsilon$ = -9.8, -7.5, -5, -3.5, -2 at 1 kHz) were selected to characterize the light efficiency of FFS devices with various cell gaps and rubbing directions.

III. RESULTS AND DISCUSSION

Figure 2(a) shows voltage dependent transmittance curves for different values of the positive dielectric anisotropy ($\Delta\epsilon$ = 2, 5, 9.4, 13) while keeping the other conditions such as the rubbing angle and the cell gap, the same. The variations in the maximum transmittance and the operating voltage with dielectric anisotropy are illustrated in Fig. 2(b). The transmittance and the operating voltage gradually decrease with increasing $\Delta\epsilon$ values. The transmittance for $\Delta\epsilon$ = 5 (LC1) was found to be about 7% higher than it was for $\Delta\epsilon$ = 9.4 (LC2).

Figure 3 shows the LC orientation at three different electrode positions, A, B, and C, and the transmittance along the y axis in the white state. As indicated in Fig. 3, the tilt angle at position B is larger than those at the other two positions A and C. According to Eq. (5), increasing $\Delta\epsilon$ would also increase the $F_{electric}$, which in turn reduces Gibbs free energy. Because of the decrease in the Gibbs energy function, the molecules will be tilted easily for higher value of $\Delta\epsilon$. Therefore, LC2 would have a higher tilt angle at position B than LC1. The user tilt angle of the LC at position B gives rise to a less elastic torque on the LC at position C so that the twisted angle of the LC at position C is smaller in the LC with a higher tilt angle. Because of the lower elastic torque due to the large $\Delta\epsilon$, the LC molecules at the center (at C) would not be twisted as much by their neighboring

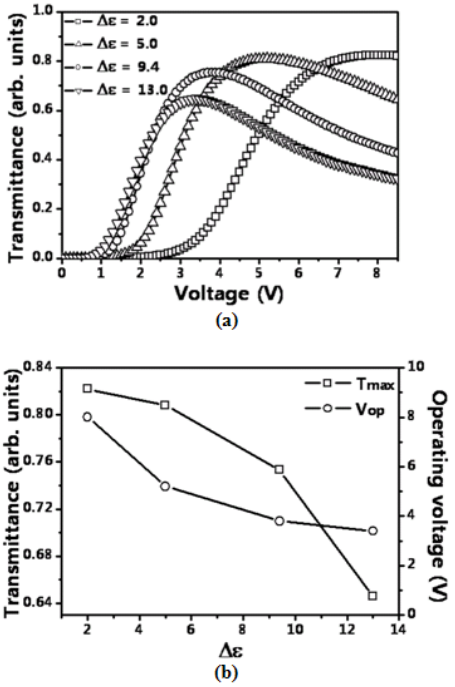

Fig. 2. (a) Voltage-dependent transmittance curves and (b) maximum transmittance and operating voltage with +LC as a fanction of the magnitude of $\Delta\epsilon$.

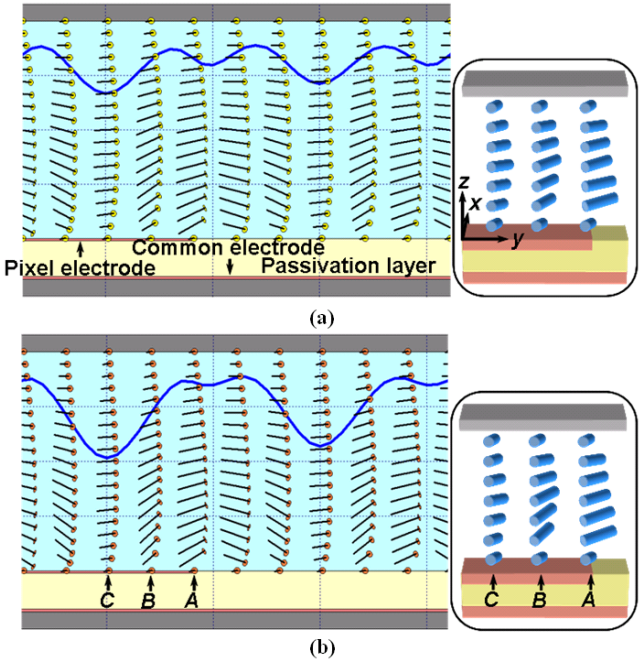

Fig. 3. LC orientations and transmittance according to the electrode positions showing different tilts and twists angle above the electrode, wheel depend on the magnitude of $\Delta\epsilon$ in the on-state: (a) $\Delta\epsilon$ = 5.0 and (b) $\Delta\epsilon$ = 9.4.

molecules as they would for low values of $\Delta\epsilon$. Hence, the LC with $\Delta\epsilon$ = 5 would have a lower tilt angle at position

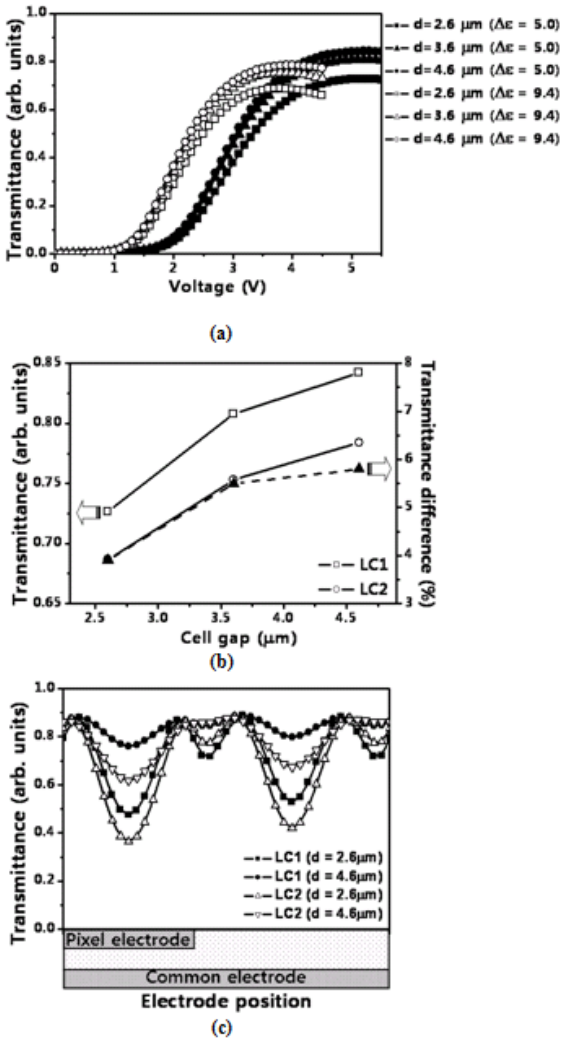

Fig. 4. (a) Voltage-dependent transmittance curves, (b) transmittance and transmittance difference between two +LCs as functions of the cell gap, and (c) electrode-position-dependent transmittance between two +LCs for two different cell gaps.

B, the LC molecules at position C would be twisted more by their neighboring molecules than they would for $\Delta\epsilon$ = 9.4. As a result, the twist angle Ψ at position C, for $\Delta\epsilon$ = 9.4 would be lower than that for $\Delta\epsilon$ = 5, as depicted in Fig 3. In the case of position B, the higher tilt angle decreases the effective dΔn. Hence, according to Eq. (2) the transmittance at positions B and C would be lower for higher value of $\Delta\epsilon$ due to decreases in the effective retardation (at B) and the twist angle (at C), respectively. However, the transmittance at position A is almost the same for both LCs, as shown in Fig. 3. Consequently the resultant transmission is found to be higher for lower values of $\Delta\epsilon$ (see Fig. 2).

Figure 4(a) illustrates the voltage-dependent transmittance curve for +LC as s function of the cell gap for LC1 and LC2. As shown in the Fig. 4(a), the transmittance decreases with increasing $\Delta\epsilon$ for the same values of the cell gap, as explained above. However, the transmittance increases with increasing in cell gap [16]. The transmittance difference for LC1 and LC2 with increasing in cell gap is shown in Fig. 4(b). As clearly illustrated, the transmittance difference between LC1 and LC2 is 3.9% when $d = 2.6$ μm, but it increases to 5.8% when the cell gap increases to 4.6 μm. This indicates that the structures having larger cell gaps are more affected by the magnitude of $\Delta\epsilon$. Further, as the observed transmission in the case of LC2 is smaller than that of LC1, the increasing rate of transmittance with increasing cell gap is smaller in LC2 than it is in LC1. In order to investigate the above-mentioned tendency of the transmittance, we a lot the transmittance as a function of the electrode positions in Fig. 4(c). As clearly indicated in Fig. 4(c), the transmittance difference mainly occurs at position C and increases with increasing cell gap. Moreover, the transmittance difference between two cells with $d = 2.6$ μm and $d = 4.6$ μm at position C is higher in LC1 than in LC2.

In addition, the transmittance of the FFS mode also depends on the rubbing angle, where is the angle between the LC director and the horizontal component of the fringe electric field [11]. Figure 5(a) shows voltage-dependent transmittance curves for LC1 and LC2 for various rubbing angles. As indicated, the transmittance increases whereas driving voltage decreases with increasing rubbing angle in both cells. Due to the decreasing driving voltage with increasing rubbing angle, the dielectric torque will be decreased; hence, the tilt angle of the LC molecules will be low, which, in turn, increases the transmission of the FFS mode, as explained earlier. To find the effect of a change in the rubbing angle on the transmittance, we calculated the transmittance difference for LC1 and LC2 for various rubbing angles, as shown in Fig. 5(b). From Fig. 5(b), the transmittance differences between LC1 and LC2 drops with increasing rubbing angle. As the driving voltage and the tilt angle of LC molecules increases with decreasing rubbing angle, LC2, which has a higher tilt angle due to its high $\Delta\epsilon$ compared to LC1, has much lee way with increasing rubbing angle scope to tilt down until its saturation level. Therefore, the degree of increase in the transmission in LC2 will be steeper than in LC1 with increasing rubbing angle. Further, the transmission of LC2 is lower than that of LC1, as already discussed. Consequently, the transmittance differences between LC1 and LC2, 7.6% at a rubbing angle of 74°, drops to 3.8% with increasing rubbing angle to 86°, as shown in Fig. 5(b). The electrode position dependent transmittances for LC1 and LC2 for two different rubbing angles are shown in Fig. 5(c). As clearly illustrated in Fig. 5(c), with various rubbing angle, the difference in the transmittance is mainly decided by the pixel electrode position C, for which the twist angle is determined by the elastic torque between neighboring molecules of position B. From the above results, one can understand that such an electro-optic difference de-

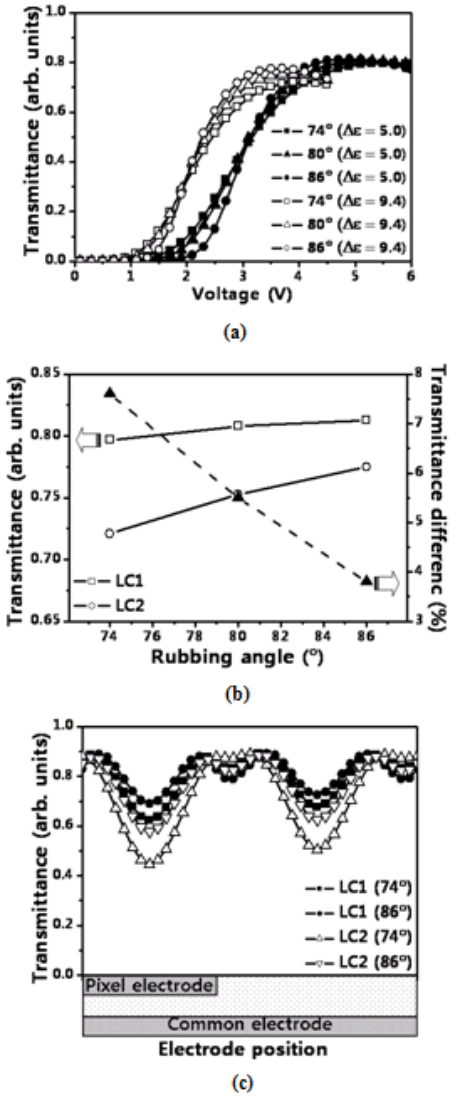

Fig. 5. (a) Voltage-dependent transmittance curves, (b) transmittance and transmittance difference between two +LCs as functions of the rubbing angle, and (c) electrode-position-dependent transmittance between two +LCs for two different rubbing angles.

pending on the magnitudes of the dielectric anisotropy, the cell gap, and the rubbing angle mainly comes from the molecular orientation around electrode position C, whose orientation is determined by the correlation with neighboring molecules.

The +LC will try to orient parallel to the field; however, the –LC orients perpendicular to the electric field. In other words, the +LC will tilt upward highly along the fringe field at electrode position B whereas the fringe field at that position will generate much less tilt angle with –LC that with +LC. Therefore, in order to understand clearly how the observed electro-optic characteristics with +LC might be changed with –LC, we performed an investigations with –LC.

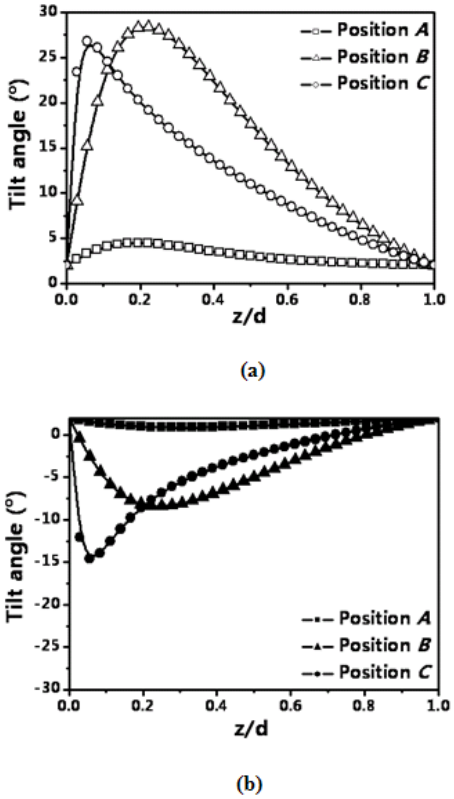

Fig. 6. Profiles of the tilt angles at three electrode positions for different to signs of the LC dielectric anisotropy: (a) +LC with $\Delta\epsilon = 5.0$ and (b) –LC with $\Delta\epsilon = -5.0$.

First of all, the profiles of the tilt angle alongs the LC layer at three electrode positions for +LC and –LC in the white state ware studied. As clearly indicated in Fig 6, +LC shows a higher tilt angle that –LC at all electrode positions. To understand the difference in detail, we calculated the average tilt angle. As a result, +LC has a tilt angle of 9.7° (at A), 13.2° (at B), and 1.0° (at C) while –LC has a tilt angle of -5.4° (at A), -5.4° (at B), and –0.7° (at C) from the original tilt angle of 2° Here "–" indicates that the tilt deformation occurs in a direction opposite to the initial tilt direction. Because of the low tilt angle generated by the field, the FFS cell with –LC shows a higher transmittance than the FFS cell with +LC [6].

In order to confirm the tendency of the transmittance as a function of the magnitude of $\Delta\epsilon$ in –LC compared to +LC, we calculated the transmittance as a function of the magnitude of $\Delta\epsilon$ for –LC, as shown in Fig. 7. As indicated, the transmittance increases slightly with decreasing magnitude of $\Delta\epsilon$, but the difference in transmittance is not as strong as it is for +LC. This indicates that for –LC in the FFS cell, the degree of tilt angle at electrode position B does not depend much on the magnitude of $\Delta\epsilon$. As a result, the cell gap and the rubbing angle is not as strong as it is for dependency of the magnitude of $\Delta\epsilon$ the +LC.

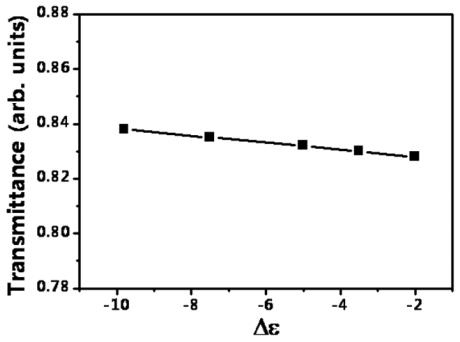

Fig. 7. Maximum transmittance as a function of magnitude of the $\Delta\epsilon$ for –LC.

IV. SUMMARY

In this research, we studied how the light efficiency of the FFS mode depended on the magnitude of $\Delta\epsilon$ for positive and negative dielectric anisotropy. The results show that the transmittance can be greatly increased by using a low-dielectric anisotropy +LC and that the, transmittance for different values of $\Delta\epsilon$ is highly influenced for the cell by a high cell gap and a low rubbing angle. However, for –LC, the magnitude of $\Delta\epsilon$ does not affect the transmittance, such as the cell gap and the rubbing angle, should be considered for the light efficiency and for the proper operating voltage whereas when choosing the magnitude of for –LC, the operating voltage should mainly be considered. The results give new information on understanding the electro-optic characteristics of the FFS mode to maximize the light efficiency.

ACKNOWLEDGMENTS

This work was supported by Merck Advanced Technology Korea, by the World Class University program through Ministry of Education, Science and Technology all rights reserved (R31-2008-000-20029-0), and by Selection of Research-oriented Professor Program of Chonbuk National University in 2009.

REFERENCES

[1] A. Takeda, S. Kataoka, T. Sasaki, H. Chida, H. Tsnda, K. Ohmuro, Y. Koike, T. Sasabayashi and K. Okamoto, SID Int. Symp. Dig. Tech. Pap. **29**, 1077 (1998).

[2] S. S. Kim, K. H. Kim, B. Berkeley and T. Kim, Proc. 26th Int. Display Research Conf. (Kent, OH, USA, 2006), p. 154.

[3] B. Kiefer, B. Weber, F. Windsceid and G. Baur, Proc. 12th Int. Display Research Conf. (Hiroshima, Japan, 1992), p. 547.

[4] M. Oh-e and K. Kondo, Appl. Phys. Lett. **67**, 3895 (1995).

[5] I. S. Song, I. S. Baik, T. M. Kim, S. H. Lee, D. S. Kim, H. S. Soh and W. Y. Kim, J. Inf. Display **5**, 18 (2004).

[6] S. H. Lee, S. L. Lee and H. Y. Kim, Appl. Phys. Lett. **73**, 2881 (1998).

[7] S. H. Lee, S. L. Lee, H. Y. Kim and T. Y. Eom, SID Int. Symp. Dig. Tech. Pap. **30**, 202 (1999).

[8] S. H. Lee, S. M. Lee, H. Y. Kim, J. M. Kim, S. H. Hong, Y. H. Jeong, C. H. Park, Y. J. Choi, J. Y. Lee, J. W. Koh and H. S. Park, SID Int. Symp. Dig. Tech. Pap. **32**, 484 (2001).

[9] S. H. Lee, H. Y. Kim, S. M. Lee, S. H. Hong, J. M. Kim, J. W. Koh, J. Y. Lee and H. S. Park, J. Soc. Inf. Disp. **10**, 224 (2002).

[10] I. Mori, R. Oke, K. Kamoshida, T. Asakura and K. Ono, Proc. 25th Int. Display Research Conf. (Edinburgh, Scotland, 2005), p. 102.

[11] S. H. Hong, I. C. Park, H. Y. Kim and S. H. Lee, Jpn. J. Appl. Phys. **39,** L527 (2000).

[12] S. H. Lee, S. L. Lee, H. Y. Kim and T. Y. Eom, J. Kor. Phys. Soc. **35,** S1111 (1999).

[13] Y. J. Lim, M. H. Lee, G. D. Lee, W. G. Jang and S. H. Lee, J. Phys. D: Appl. Phys. **40**, 2759 (2007).

[14] S. H. Jung, H. Y. Kim, J. H. Kim S. H. Nam and S. H. Lee, Jpn. J. Appl. Phys. **43**, 1028 (2004).

[15] S. M. Oh, S. J. Kim, M. H. Lee, D. S. Seo and S. H. Lee, Mol. Cryst. Liq. Cryst. **433**, 97 (2005).

[16] S. H. Jung, H. Y. Kim, M-H. Lee, J. M. Rhee and S. H. Lee, Liq. Cryst. **32**, 267 (2005).

[17] S. J. Kim, H. Y. Kim, S. H. Lee, Y. K. Lee, K. C. Park and J. Jang, Jpn. J. Appl. Phys. **44**, 6581 (2005).

[18] H. Y. Kim, S-H. Nam and S. H. Lee, Jpn. J. Appl. Phys. **42**, 2752 (2003).

[19] J. W. Ryu, J. Y. Lee, H. Y. Kim, J. W. Park, G-D. Lee and S. H. Lee, Liq. Cryst. **35**, 407 (2008).

[20] H. Y. Kim, G. R. Jeon, D-S. Seo, M-H. Lee and S. H. Lee, Jpn. J. Appl. Phys. **41**, 2944 (2002).

[21] S. H. Hwang, Y. J. Lim, M-H. Lee, S. H. Lee, G-D. Lee, H. K., H. Kang, K. J. Kim and H. C. Choi, Curr. Appl. Phys. **7**, 690 (2007).

[22] A. Lien, Appl. Phys. Lett. **57,** 2767 (1990).